processes

MDPI

Article

Energy Analysis of the S-CO_2 Brayton Cycle with Improved Heat Regeneration

Muhammad Ehtisham Siddiqui * and Khalid H. Almitani

Mechanical Engineering Department, King Abdulaziz University, Jeddah 21589, Saudi Arabia; kalmettani@kau.edu.sa

* Correspondence: mesiddiqui@kau.edu.sa or ehtisham.siddiqui@gmail.com; Tel.: +966-55-218-4681

Received: 28 November 2018; Accepted: 17 December 2018; Published: 20 December 2018

Abstract: Supercritical carbon dioxide (S-CO_2) Brayton cycles (BC) are promising alternatives for power generation. Many variants of S-CO_2 BC have already been studied to make this technology economically more viable and efficient. In comparison to other BC and Rankine cycles, S-CO_2 BC is less complex and more compact, which may reduce the overall plant size, maintenance, and the cost of operation and installation. In this paper, we consider one of the configurations of S-CO_2 BC called the recompression Brayton cycle with partial cooling (RBC-PC) to which some modifications are suggested with an aim to improve the overall cycle's thermal efficiency. The type of heat source is not considered in this study; thus, any heat source may be considered that is capable of supplying temperature to the S-CO_2 in the range from 500 °C to 850 °C, like solar heaters, or nuclear and gas turbine waste heat. The commercial software Aspen HYSYS V9 (Aspen Technology, Inc., Bedford, MA, USA) is used for simulations. RBC-PC serves as a base cycle in this study; thus, the simulation results for RBC-PC are compared with the already published data in the literature. Energy analysis is done for both layouts and an efficiency comparison is made for a range of turbine operating temperatures (from 500 °C to 850 °C). The heat exchanger effectiveness and its influence on both layouts are also discussed.

Keywords: supercritical carbon dioxide; recompression Brayton cycle; partial cooling; improved heat regeneration; thermal efficiency; energy analysis; heat exchanger effectiveness

1. Introduction

Rapid technological advancements and increasing industry all around the world have significantly increased the demand of energy. On the other side, fossil reserves are depleting rapidly, resulting in global warming and issues relating to environmental pollution. Because of this, the development of more efficient power cycles needs attention. One step towards efficiency improvement may be the utilization of industrial waste heat [1]. The supercritical carbon dioxide (S-CO_2) Brayton cycle (BC) has been extensively studied in the last decade and is considered promising for exploiting low- to medium-grade heat for power generation [2]. No commercial S-CO_2 power plant has yet been installed; however, some pilot small-scale units are currently present [3–5].

Carbon dioxide as a working fluid is non-toxic, stable, and non-combustible [2]. A power block utilizing S-CO_2 has many benefits due to its compactness, low maintenance and running costs, and structural simplicity [6,7]. Another advantage which makes the utilization of CO_2 worthy in supercritical BC is the rapid change in its thermo-physical properties near its critical point. The density of CO_2 near its critical point is similar to that of its liquid form and reduces the compressor work significantly. Secondly, S-CO_2 is almost twofold as dense as steam, resulting in a power block with high power density in comparison to the steam Rankine cycle (RC). Aside from certain benefits, RC has many disadvantages over S-CO_2, like poor thermal efficiency due to phase change and huge plant size.

Feher [8] and Angelino [9] proposed the supercritical carbon dioxide cycle in the 1960s. They achieved a cycle thermal efficiency of close to 55% under ideal conditions. However, this cycle came back into the limelight in 2004 after the refined version was proposed by Dostal [10] with its application to next-generation nuclear reactors. Since then, different configurations for the S-CO_2 Brayton cycle have been reported in the literature, including the simple cycle, the pre-compression cycle, the re-compression cycle with a partial cooling cycle, the intercooling cycle, and the split expansion cycle [11,12].

The integration of various types of heat sources into S-CO_2 BC has been studied in the last decade. Sarkar [13] performed an energy and exergy analysis of the S-CO_2 recompression Brayton cycle (RBC) utilizing nuclear waste heat and performed a sensitivity analysis. He concluded that the irreversibilities of heat exchangers are considerably greater in comparison to those of turbo-machineries. Sarkar and Bhattacharyya [14] performed an exergy analysis for the RBC and optimized its performance. They found that the differences in specific heat capacities at the compressor outlet and the turbine outlet play an important role in the optimization of the cycle's pressure ratio and intermediate pressure. Ahn et al. [15] investigated various configurations of the S-CO_2 BC for application to nuclear reactors and identified an RBC layout more efficient for a mild turbine inlet temperature range (450 °C to 600 °C).

The integration of concentrating solar power (CSP) with S-CO_2 Brayton cycles has also been investigated. Turchi [16] studied an S-CO_2 RBC integrated with CSP and found that it could offer efficiencies higher than those of supercritical or superheated steam Rankine cycles. Padilla [17] performed an energy and exergy analysis of eight different configurations of S-CO_2 with the heat source being a solar receiver. He concluded that the recompression Brayton cycle with main compressor intercooling has the best thermal and exergetic performance. This was achieved by introducing an intercooling stage in the main compressor, which is claimed to decrease the compressor work and, eventually, the net power output of the cycle. The literature also reports the utilization of cold energy of liquefied natural gas (LNG) as a heat sink in proposing new configurations for the CO_2 power cycle with an ultimate goal of improving the thermodynamic performance of the cycle [18–21].

The literature reports numerous thermodynamic analyses carried out for S-CO_2 power cycles utilizing either waste heat, nuclear, or CSP systems. Various configurations have been proposed to achieve the maximum possible thermal efficiencies. In this paper, we propose modifications to the standard recompression Brayton cycle with partial cooling (RBC-PC) which target maximum recovery of heat from within the cycle to minimize external heat input, thus maximizing the overall cycle's thermal efficiency. No specific type of heat input to the cycle is considered; thus, the proposed configuration may be integrated with any suitable heat source working within the range of the turbine inlet temperature of interest. The effect of heat exchanger effectiveness on the cycle's performance is also examined for both configurations.

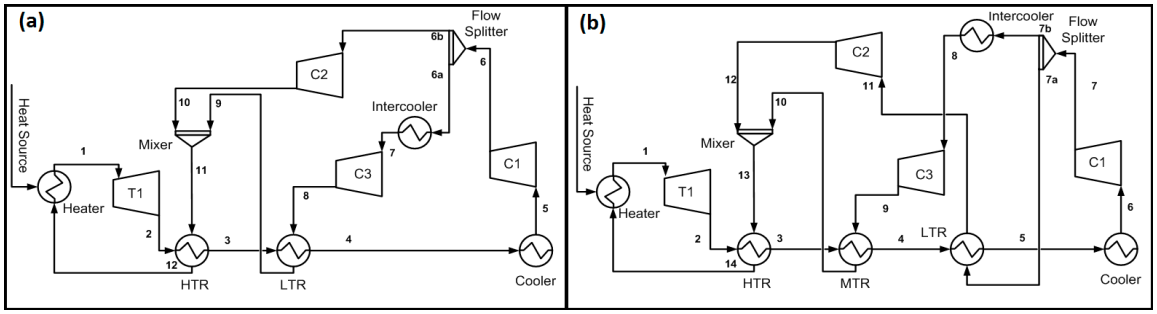

Figure 1. Supercritical CO_2 (S-CO_2) power cycle layouts: (**a**) recompression Brayton cycle (RBC) with partial cooling and (**b**) RBC with partial cooling and improved heat regeneration. LTR: low-temperature recuperator; HTR: high-temperature recuperator. Layouts (**a**) adapted from [17].

2. Cycle Configurations

In this paper, we investigate two variants of S-CO_2 Brayton cycles. One is the recompression Brayton cycle with partial cooling (RBC-PC), and the second is the modified version of RBC-PC with improved heat regeneration (RBC-PC-IHR). Many researchers have already studied the RBC-PC [11,16,17]; thus, it can serve as a basis for comparison of the proposed layout performance. Figure 1 presents the configurations of both cycles.

Figure 1a presents the layout of the RBC with partial cooling. In this configuration, the stream leaving low-temperature recuperator (State 4), denoted by LTR, is cooled and compressed (State 6) to the intermediate pressure of the cycle using main compressor C1. The stream is then divided into two; one is cooled and compressed to the high pressure of the cycle (State 8) which later recovers heat in LTR, whereas the second stream is compressed to the high pressure of the cycle (State 10) and mixed with the first stream leaving LTR (State 9). The mixed stream (State 11) recovers heat in high-temperature recuperator (HTR) and then flows to the heat source, where it is heated to the cycle's high temperature. The high-temperature and high-pressure stream (State 1) is expanded in the expander (T1).

Figure 1b presents the proposed configuration (RBC-PC-IHR); it is very similar to the RBC-PC but with a third heat recuperator for improved heat regeneration. In this configuration, the stream leaving the LTR (State 5) is cooled (State 6) and compressed (State 7) to the intermediate pressure of the cycle. The stream is then divided into two; one stream (stream 7b) is cooled and compressed to the cycle's high pressure, then flows to a medium-temperature recuperator (MTR) to recover the heat, whereas the other stream (stream 7a) receives heat in LTR before it is compressed to the high pressure of the cycle in C2. The streams leaving the compressor C2 and MTR are mixed and flow to HTR to recover heat before heating in the Heater.

Figure 2a,b display the temperature–entropy plots for the RBC-PC and RPC-PC-IHR, respectively, at a turbine inlet temperature of 500 °C. In the proposed layout (RBC-PC-HR), the S-CO_2 stream after the compression process between States 6 and 7 splits into two; one is cooled down to State 8, and the second recovers heat in LTR and reaches State 11 prior to compression between States 11 and 12. Because of the heat recuperation in LTR (between States 7 and 11), the temperature of the S-CO_2 prior to HTR (between States 13 and 14) is higher than that which could be achieved at the same location in RBC-PC. Eventually, due to higher heat recuperation with the RBC-PC-IHR layout, the temperature of the S-CO_2 before the heat source is higher in RBC-PC-IHR, which requires less heat input in the Heater in comparison to the RBC-PC layout.

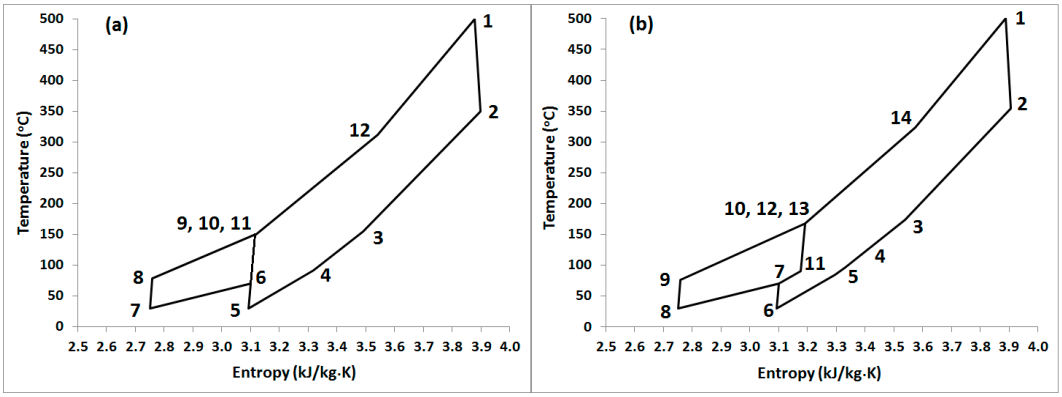

Figure 2. A temperature–entropy diagram for different S-CO_2 Brayton cycle layouts: (**a**) RBC-PC, and (**b**) RBC-PC with improved heat regeneration (RBC-PC-IHR). The highest temperature of the cycle is 500 °C.

3. Energy Model

The first-law efficiency, the thermal efficiency (η_{th}), of the cycle is calculated as

$$\eta_{th} = (\dot{W}_{turbine} - \dot{W}_{net,\ compressor}) / (\dot{Q}_{heater}) \quad (1)$$

where $\dot{W}_{turbine}$ is the work output of the turbine and $\dot{W}_{net,\ compressor}$ is the net compression work input to the cycle. $\dot{Q}_{heater}$ is the heat input given to the cycle via the heat source. The heat exchanger effectiveness, η_{HEX}, is considered for the total hot stream [17,22] and is defined as

$$\eta_{HEX} = (h_{HTR\_HI} - h_{LTR\_HO}) / (h_{HTR\_HI} - h_{LTR\_HO@Tc}) \quad (2)$$

where h_{HTR_HI} and h_{LTR_HO} are the enthalpies of the hot streams at the inlet of the high-temperature recuperator and the outlet of the low-temperature recuperator, respectively. $h_{LTR\_HO@Tc}$ is the enthalpy of the hot stream at the outlet of the low-temperature recuperator calculated based on the minimum temperature that it could achieve [23] (T_8 for RBC-PC and T_7 for RBC-PC-IHR). Since in both configurations the flow stream splits into two, another important parameter called the split ratio (SR) is introduced, which is defined as the ratio of mass flow rate of the cold stream entering LTR to the total mass flow rate of the cycle. It is equal to $\dot{m}_{6a}/\dot{m}_t$ for RBC-PC and $\dot{m}_{7a}/\dot{m}_t$ for RBC-PC-IHR, where $\dot{m}_t$ is the cycle's total mass flow rate.

4. Simulation Environment

The commercial software Aspen HYSYS V9 (Aspen Technology, Inc., Bedford, MA, USA) was used to configure and simulate the S-CO_2 Brayton cycles. We used the Peng–Robinson model for the state properties calculation. The investigation assumes the following conditions:

1. The cycle operates under steady-state conditions [11,16,17];
2. Energy losses in the pipelines are negligible [11,16,17];
3. The compression and expansion processes are adiabatic [11,16,17];
4. The turbine and compressor efficiencies are 93% and 89%, respectively [11,16,17];
5. The heat exchanger effectiveness is 95% (except in Section 7.2, where we investigate its effect on cycle performance) with a minimum pinch point temperature (ΔT_{min}) of 5 °C for all heat exchangers [11,16,17];
6. The cycle maximum pressure is 25 MPa [11,16,17];
7. The turbine inlet temperature varies from 500 °C to 850 °C;
8. The cycle intermediate pressure is 7.5 MPa;
9. The split ratio (SR) is 0.5.

5. Parametric Adjustments

The thermodynamic performance of S-CO_2 recompression Brayton cycles is greatly influenced by a number of parameters, such as the turbine inlet temperature, cycle pressure ratio, split ratio, heat exchanger effectiveness, and the minimum allowed temperature in the heat exchangers [8–10,24,25]. To compare our results with the published data, we kept some of the parameters constant, as mentioned in Section 4. Some parameters were adjusted to operate the cycle at near-optimal conditions. We investigated the performance of each configuration, shown in Figure 1, against the cycle's minimum pressure, p_{min}, (p_5 for RBC-PC and p_6 for RBC-PC-IHR). The turbine inlet pressure (TIP) values considered were 16 MPa and 25 MPa (which is the maximum allowable in this study).

Figure 3 presents the cycle's thermal efficiency and minimum pinch temperature plotted against the cycle's minimum pressure for RBC-PC and RCB-PC-IHR. Considering RBC-PC (Figure 3a) with a turbine inlet temperature of 850 °C, the cycle's thermal efficiency decreases continuously with the increase of p_{min} for a turbine inlet pressure of 16 MPa or 25 MPa, whereas the minimum allowable

pinch temperature (ΔT_{min}), i.e., 5 °C, occurs at p_{min} close to 3.8 MPa for a TIP of 25 MPa. For a turbine inlet temperature of 500 °C with a TIP of 25 MPa, the temperature remains crossed in the heat exchanger. However, with a TIP of 16 MPa, the minimum pinch temperature of 5 °C occurs for p_{min} approximately equal to 4.3. Thus, the cycle's minimum pressure (p_5) was set to 4.5 MPa for RBC-PC. Similarly, the near-optimal value of the cycle's minimum pressure was set to 5.5 MPa for RBC-PC-IHC.

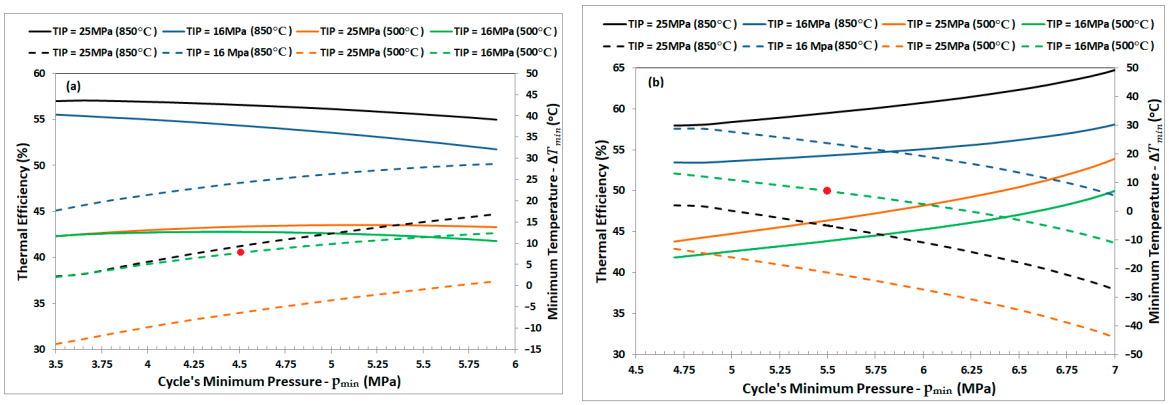

(**a**) (**b**)

Figure 3. Cycle thermal efficiency (solid lines) and minimum pinch temperature in the heat exchanger (dashed lines) plotted as a function of the cycle's minimum pressure (p_{min}) for (**a**) RBC-PC and (**b**) RBC-PC-IHR. The turbine inlet pressure (TIP) was set to 25 MPa or 16 MPa for turbine inlet temperatures (TIT) of 850 °C and 500 °C. The red dot shows the near-optimal value for the cycle's minimum pressure.

6. Model Validation

The simulation results for the base cycle, i.e., RBC-PC, were validated using data already published by Kulhánek and Dostál [11], Turchi et al. [16], and Padilla et al. [17]. Figure 4 presents the effect of the turbine inlet pressure on the efficiency and minimum pinch temperature at different turbine inlet temperatures from 500 °C to 850 °C. The thermal efficiency increases monotonically with increasing turbine inlet pressure and temperature, as shown in Figure 4a. For a given turbine inlet temperature, the minimum pinch temperature decreases linearly for a turbine inlet pressure above 16 MPa, as shown in Figure 4b. Thus, for a given turbine inlet temperature, the maximum cycle efficiency is restricted by the condition of the minimum allowable pinch temperature. In the current study, the minimum pinch temperature is 5 °C; thus, the red dots in Figure 4b represent the near-optimal operating pressures for each turbine inlet temperature, and their values are listed in Table 1. Figure 5 presents a plot of the thermal efficiency of the cycle versus turbine inlet temperatures. Data points taken from references [11,16,17] are also plotted for comparison. It is evident from the plots that the results produced by the current model agree well with those in the literature. Slight differences between our data and published data could be a result of differences in the thermodynamic properties databases used in this simulation and in published models.

Table 1. Turbine inlet pressures at different turbine inlet temperatures for maximum thermal efficiency of the recompression Brayton cycle with partial cooling (RBC-PC).

Turbine inlet temperature (°C)	500	550	600	650	700	750	800	850
Turbine inlet pressure (MPa)	20.0	21.5	23.0	24.9	25.0	25.0	25.0	25.0
Thermal efficiency (%)	43.2	45.7	48.0	50.0	51.7	53.2	54.5	55.8

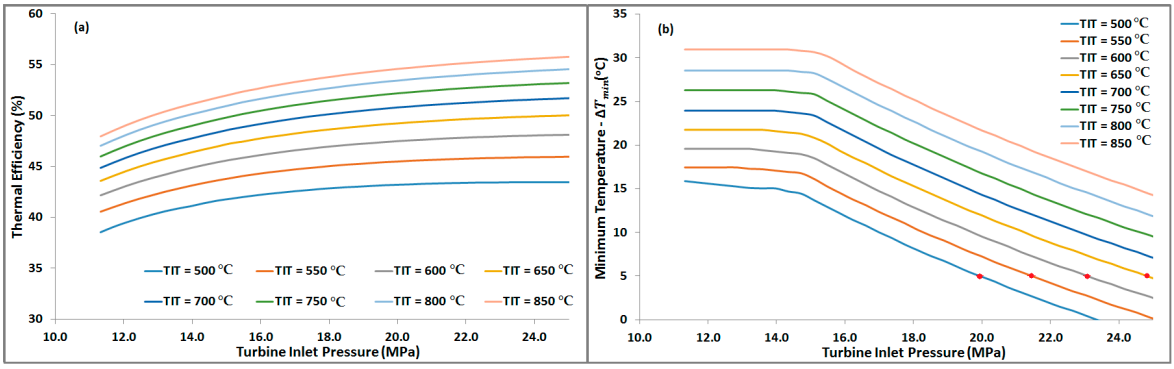

Figure 4. (**a**) Thermal efficiencies of RBC-PC plotted versus turbine inlet pressure for TIT from 500 °C to 850 °C. (**b**) Minimum pinch temperature versus turbine inlet pressure; red dots represent the minimum pinch temperature of 5 °C.

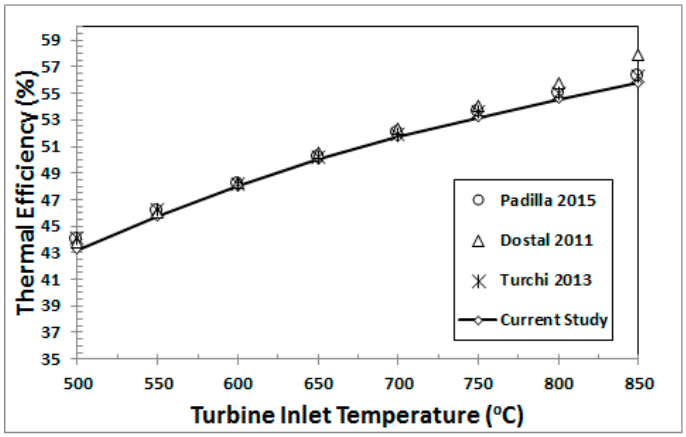

Figure 5. Validation of simulation results for the RBC-PC with [11,16,17].

7. Results and Discussions

7.1. Cycle Thermal Efficiency

The performance of the proposed cycle, RBC-PC-IHR, was studied by comparing its thermal efficiency with that of RBC-PC. Figure 6 shows the variation in the proposed cycle's thermal efficiency and minimum pinch temperature in the heat exchanger with respect to the turbine inlet pressure for a range of turbine inlet temperatures. The cycle efficiency increases monotonically with increasing turbine inlet pressure and temperature, as expected. The minimum pinch temperature in the heat exchangers also drops with increasing turbine inlet pressure, thus limiting the maximum possible operating pressure of the cycle. Table 2 lists the near-optimal values of turbine operating pressures at different turbine inlet temperatures with a minimum pinch temperature of 5 °C.

Table 2. Turbine inlet pressures at different turbine inlet temperatures for maximum thermal efficiency of the RBC-PC with improved heat regeneration (RBC-PC-IHR).

Turbine inlet temperature (°C)	500	550	600	650	700	750	800	850
Turbine inlet pressure (MPa)	17.2	17.9	18.6	19.3	20	20.7	21.4	22.1
Thermal efficiency (%)	44.1	46.8	49.2	51.4	53.3	55.0	56.7	58.2

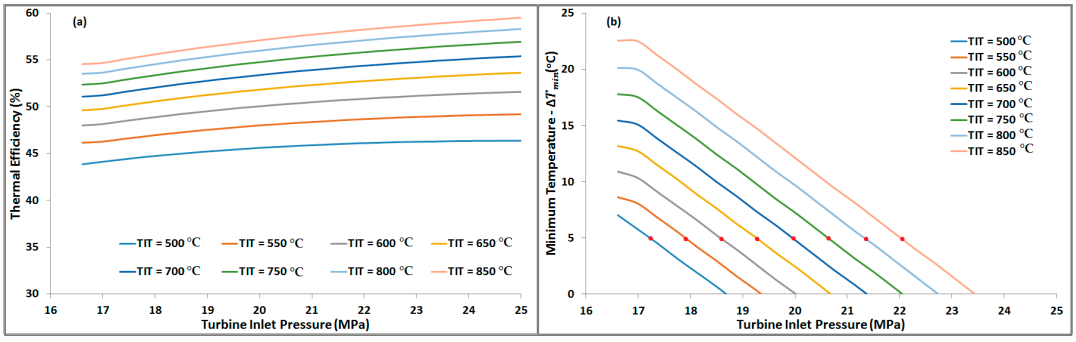

Figure 6. (**a**) Thermal efficiencies of the RBC-PC-IHR plotted versus turbine inlet pressure for TIT from 500 °C to 850 °C. (**b**) Minimum pinch temperature versus turbine inlet pressure; red dots represent the minimum pinch temperature of 5 °C.

The thermal efficiency of the RBC-PC-IHR configuration is plotted in Figure 7a along with the efficiency of the RBC-PC at different turbine inlet temperatures. A significant increase in thermal efficiency for the RBC-RC-IHR configuration is noted, especially at high turbine inlet temperatures. Figure 7b is plotted to compare the efficiency improvement (in percentage points) offered by the RBC-PC-IHR layout in comparison to the RBC-PC. A minimum efficiency increase of 2% occurs at a turbine inlet temperature of 500 °C, and this increases to nearly 4.5% by 800 °C.

Besides being more efficient, the RBC-PC-IHR operating pressure is much lower than that for the RBC-PC configuration (refer to Tables 1 and 2). For both cycles, the operating turbine inlet pressure increases with increasing turbine inlet temperature with a minimum of 20 MPa and 17.2 MPa at a turbine inlet temperature of 500 °C for RBC-PC and RBC-PC-IHR, respectively. The maximum pressure is restricted to 25 MPa in this investigation, which is attained by RBC-PC at the turbine inlet temperature of 700 °C; however, for the RBC-PC-IHR configuration, the turbine inlet pressure is raised up to 22.1 MPa by the turbine inlet temperature of 850 °C.

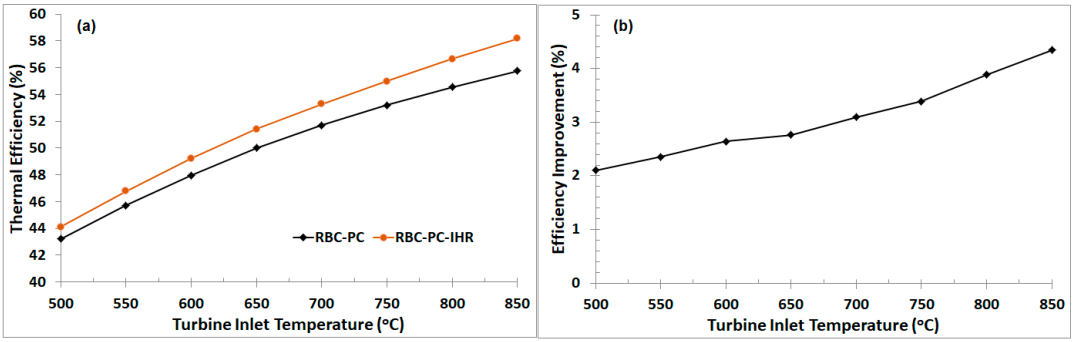

Figure 7. (**a**) The thermal efficiencies of RBC-PC-IHR and RBC-PC plotted versus turbine inlet temperatures from 500 °C to 850 °C. (**b**) The improvement in thermal efficiency from RBC-PC-IHR compared to RBC-PC in percentage points.

7.2. Heat Exchanger Effectiveness

An investigation was carried out to evaluate the performance of both cycles (RBC-PC and RBC-PC-IHR) with respect to heat exchanger effectiveness (η_{HEX}). The heat exchanger effectiveness varies between 85% and 95%. For each value of heat exchanger effectiveness, the cycle minimum pressure (p_5 for RBC-PC and p_6 for RBC-PC-IHR) was adjusted following the procedure mentioned earlier in Section 5. Figure 8a presents the cycle thermal efficiency at different turbine inlet temperatures for heat exchanger effectiveness values of 85% and 95%. Decreasing the heat exchange effectiveness decreases the cycle efficiency due to a decrease in heat recuperation. The thermal efficiency of the

proposed layout (RBC-PC-IHR) at low values of heat exchanger effectiveness is significantly better than that of RBC-PC, especially at low turbine inlet temperatures.

Figure 8b presents an estimate of the efficiency improvement offered by the RBC-PC-IHR configuration in comparison to the RBC-PC at different values of heat exchanger effectiveness. The RBC-PC-IHR configuration was found to be nearly 14% more efficient than the RBC-PC at a turbine inlet temperature of 500 °C. Except for a heat exchanger effectiveness of 95%, with increasing turbine inlet temperature, a fall in efficiency improvement is noticed with a minimum of nearly 5% at a turbine inlet temperature of 850 °C.

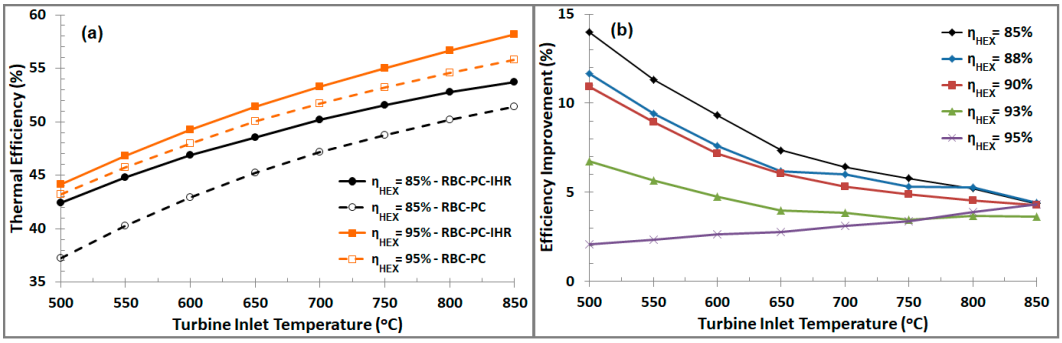

Figure 8. (**a**) Cycle thermal efficiencies versus turbine inlet pressure with heat exchanger effectiveness values of 85% and 95%. (**b**) Improvement in thermal efficiency from the RBC-PC-IHR compared to the RBC-PC in percentage points at different values of heat exchanger effectiveness between 85% and 95%.

8. Conclusions

In this work, we proposed a modified version of a recompression Brayton cycle with partial cooling (RBC-PC). We called this configuration a recompression Brayton cycle with partial cooling and improved heat regeneration (RBC-PC-IHR). Energy analysis was performed to investigate the thermal efficiency of the proposed cycle configuration over that of RBC-PC. The key outcomes of the investigation are as follows:

- For a given turbine inlet temperature, the thermal efficiency increased with increasing turbine inlet pressure for both configurations (RBC-PC and RBC-PC-IHR); however, the pinch temperature in the heat exchanger maintained a decreasing trend.
- For a given heat exchanger effectiveness and minimum allowable pinch temperature, the maximum turbine inlet pressure increased with increasing turbine inlet temperature for both layouts.
- The RBC-PC-IHR configuration was significantly efficient in comparison with the RBC-PC. The magnitude of its efficiency would be determined by a number of factors, like turbine inlet temperature, minimum pinch temperature in the heat exchanger, and its effectiveness.
- For a heat exchanger effectiveness of 95% and a minimum pinch of 5 °C, the RBC-PC-IHR was found to be 2% and 4.5% more efficient than the RBC-PC at turbine inlet temperatures of 500 °C and 850 °C, respectively.
- Decreasing the heat exchanger effectiveness and keeping the minimum pinch at a given value at 5 °C resulted in decreased cycle efficiency for both layouts. However, the RBC-PC lost cycle efficiency drastically, especially at low turbine inlet temperatures (between 500 °C to 700 °C). On the other side, the RBC-PC-IHR performed much better between the turbine inlet temperatures of 500 °C and 700 °C. With a heat exchanger effectiveness of 85%, the RBC-PC-IHR was found to be nearly 14% more efficient than the RBC-PC at 500 °C.
- For any given turbine inlet temperature, the operating turbine inlet pressure for the RBC-PC-IHR was found to be much lower than that for the RBC-PC, as seen from Tables 1 and 2. This would result in a more economical piping system for the RBC-PC-IHR configuration.

Author Contributions: M.E.S. conceived and set up the simulation in Aspen HYSYS V9; M.E.S. and K.H.A. analyzed the simulation results; M.E.S. wrote the article. K.H.A. managed research financials, wherever required. Both authors proofread the final submission.

Funding: This research received no external funding.

Conflicts of Interest: The authors declare no conflict of interest.

Nomenclature

TIT	turbine inlet temperature, °C
TIP	turbine inlet pressure, MPa
LTR	low-temperature recuperator
MTR	medium-temperature recuperator
HTR	high-temperature recuperator
SR	split ratio
η_{th}	thermal efficiency, %
η_{HEX}	heat exchanger effectiveness
ΔT_{min}	minimum pinch temperature, °C
p_{min}	cycle's minimum pressure, MPa
h_{HTR_HI}	enthalpy of hot stream at the inlet of high-temperature recuperator, kJ/kg
h_{HTR_HO}	enthalpy of hot stream at the outlet of low-temperature recuperator, kJ/kg

References

1. Yang, M.-H.; Yeh, R.-H. Analyzing the optimization of an organic Rankine cycle system for recovering waste heat from a large marine engine containing a cooling water system. *Energy Convers. Manag.* **2014**, *88*, 999–1010. [CrossRef]
2. Chen, Y.; Lundqvist, P.; Johansson, A.; Platell, P. A comparative study of the carbon dioxide transcritical power cycle compared with an organic Rankine cycle with R123 as working fluid in waste heat recovery. *Appl. Therm. Eng.* **2006**, *26*, 2142–2147. [CrossRef]
3. Conboy, T.; Pasch, J.; Fleming, D. Control of a Supercritical CO_2 Recompression Brayton Cycle Demonstration Loop. *J. Eng. Gas Turbines Power* **2013**, *135*, 111701. [CrossRef]
4. Conboy, T.; Wright, S.; Pasch, J.; Fleming, D.; Rochau, G.; Fuller, R. Performance Characteristics of an Operating Supercritical CO_2 Brayton Cycle. *J. Eng. Gas Turbines Power* **2012**, *134*, 111703. [CrossRef]
5. Vesely, L.; Dostal, V.; Hajek, P. Design of Experimental Loop with Supercritical Carbon Dioxide. In Proceedings of the 2014 22nd International Conference on Nuclear Engineering, Prague, Czech Republic, 7–11 July 2014; Volume 3. Next Generation Reactors and Advanced Reactors; Nuclear Safety and Security. [CrossRef]
6. Wang, X.; Dai, Y. Exergoeconomic analysis of utilizing the transcritical CO_2 cycle and the ORC for a recompression supercritical CO_2 cycle waste heat recovery: A comparative study. *Appl. Energy* **2016**. [CrossRef]
7. Santini, L.; Accornero, C.; Cioncolini, A. On the adoption of carbon dioxide thermodynamic cycles for nuclear power conversion: A case study applied to Mochovce 3 Nuclear Power Plant. *Appl. Energy* **2016**, *181*, 446–463. [CrossRef]
8. Feher, E.G. The Supercritical Thermodynamic Power Cycle. *Energy Convers.* **1968**, *8*, 85–90. [CrossRef]
9. Angelino, G. Carbon Dioxide Condensation Cycles for Power Production. *J. Eng. Gas Turbines Power* **1968**, *90*, 287. [CrossRef]
10. Dostál, V.; Driscoll, M.J.; Hejzlar, P. *A Supercritical Carbon Dioxide Cycle for Next Generation Nuclear Reactors*; Tech Rep MIT-ANP-TR-100; Massachusetts Institute of Technology: Cambridge, MA, USA, 2004; pp. 1–317.
11. Kulhánek, M.; Dostál, V. Thermodynamic Analysis and Comparison of Supercritical Carbon Dioxide Cycles. In Proceedings of the Supercritical CO_2 Power Cycle Symposium, Boulder, CO, USA, 24–25 May 2011.
12. Mahmoudi, S.M.S.; Akbari, A.D.; Rosen, M.A. Thermoeconomic Analysis and Optimization of a New Combined Supercritical Carbon Dioxide Recompression Brayton/Kalina Cycle. *Sustainability* **2016**, *8*, 1079. [CrossRef]

13. Sarkar, J. Second law analysis of supercritical CO_2 recompression Brayton cycle. *Energy* **2009**, *34*, 1172–1178. [CrossRef]
14. Sarkar, J.; Bhattacharyya, S. Optimization of recompression S-CO_2 power cycle with reheating. *Energy Convers. Manag.* **2009**, *50*, 1939–1945. [CrossRef]
15. Ahn, Y.; Bae, S.J.; Kim, M.; Cho, S.K.; Baik, S.; Lee, J.I.; Cha, J.E. Review of supercritical CO_2 power cycle technology and current status of research and development. *Nucl. Eng. Technol.* **2015**, *47*, 647–661. [CrossRef]
16. Turchi, C.S.; Ma, Z.; Neises, T.W.; Wagner, M.J. Thermodynamic Study of Advanced Supercritical Carbon Dioxide Power Cycles for Concentrating Solar Power Systems. *J. Sol. Energy Eng.* **2013**, *135*, 041007. [CrossRef]
17. Padilla, R.V.; Soo Too, Y.C.; Benito, R.; Stein, W. Exergetic analysis of supercritical CO_2 Brayton cycles integrated with solar central receivers. *Appl. Energy* **2015**, *148*, 348–365. [CrossRef]
18. Angelino, G.; Invernizzi, C.M. Carbon dioxide power cycles using liquid natural gas as heat sink. *Appl. Therm. Eng.* **2009**, *29*, 2935–2941. [CrossRef]
19. Siddiqui, M.; Taimoor, A.; Almitani, K.; Siddiqui, M.E.; Taimoor, A.A.; Almitani, K.H. Energy and Exergy Analysis of the S-CO_2 Brayton Cycle Coupled with Bottoming Cycles. *Processes* **2018**, *6*, 153. [CrossRef]
20. Deng, S.; Jin, H.; Cai, R.; Lin, R. Novel cogeneration power system with liquefied natural gas (LNG) cryogenic exergy utilization. *Energy* **2004**, *29*, 497–512. [CrossRef]
21. Zhang, N.; Lior, N. A novel near-zero CO_2 emission thermal cycle with LNG cryogenic exergy utilization. *Energy* **2006**, *31*, 1666–1679. [CrossRef]
22. Besarati, S.M.; Yogi Goswami, D. Analysis of Advanced Supercritical Carbon Dioxide Power Cycles with a Bottoming Cycle for Concentrating Solar Power Applications. *J. Sol. Energy Eng.* **2013**, *136*, 011020. [CrossRef]
23. Moran, M.J.; Shapiro, H.N.; Boettner, D.D.; Bailey, M.B. *Fundamentals of Engineering Thermodynamics*, 7th ed.; Wiley: Hoboken, NJ, USA, 2010.
24. Ahn, Y.; Lee, J.; Kim, S.G.; Lee, J.I.; Cha, J.E.; Lee, S.W. Design consideration of supercritical CO_2 power cycle integral experiment loop. *Energy* **2015**, *86*. [CrossRef]
25. Linares, J.I.; Cantizano, A.; Arenas, E.; Moratilla, B.Y.; Martín-Palacios, V.; Batet, L. Recuperated versus single-recuperator re-compressed supercritical CO_2 Brayton power cycles for DEMO fusion reactor based on dual coolant lithium lead blanket. *Energy* **2017**, *140*, 307–317. [CrossRef]